This is a corrected version of the original printed paper. The original article contained misprints due to production errors.

Induced Drag Minimization: A Variational Approach Using the Acceleration Potential

Luciano Demasi*

University of Washington, Seattle, Washington 98195-2400

A method of predicting the minimum induced drag conditions in conventional or innovative lifting systems is presented. The method is based on lifting-line theories and the small perturbation acceleration potential. Assuming linearity and rigid wake aligned with the freestream, the optimal conditions are formulated using the Euler–Lagrange integral equation subject to the conditions of fixed total lifting force and wing span. The Lagrange multiplier method is applied, and equations for the design optimum are obtained and solved directly. Particular attention is paid to the Hadamard finite-part integrals involved in the solution process. Munk's drag theorems are also applied in order to verify the quality of the solutions. In this paper, where the theoretical/computational foundation is laid for the induced drag minimization of general lifting-line configurations, the case of the biplane under optimal conditions is extensively analyzed. It is demonstrated that, under optimal conditions, the two wings (which have the same wing span) have the same circulation distribution. Cases of finite, infinite, and infinitesimal distances between the wings are analyzed as well. It is shown that the optimal distribution is, in general, not elliptical. The proposed theoretical approach is general, and it offers a valuable tool for direct prediction of minimum induced drag in both planar and nonplanar lifting systems. Results obtained by the proposed approach shed light on some of the mathematical issues involved, and they can be used for verifying results obtained by numerical math-programming-based optimization.

Nomenclature

C_{D_i} = coefficient of induced drag
$(C_{D_i})_{opt}$ = coefficient of induced drag under optimal condition
$[(C_{D_i})_{opt}]_{ref}$ = coefficient of induced drag under optimal condition for a cantilevered wing
C_L = coefficient of lift
$\bar{C}_L$ = prescribed value of the coefficient of lift
C_1, C_2 = constants
$\bar{C}$ = prescribed value of the constraint
c = auxiliary function used in the definition of the constraint
D_i = induced drag
d_j = integral of the square of the Legendre polynomial of order j
F = aerodynamic force per unit of length
F_a = aerodynamic force per unit of area
g = known function
H = distance between the two wings in a biplane
h = nondimensional distance between the two wings in a biplane
h_i = ith Gauss weight
I_{lk}^{Had} = particular Hadamrd's integral
J = functional
L = aerodynamic lift
$\bar{L}$ = prescribed value of the lift
$\bar{L}_{guess}$ = value of the lift corresponding to m_{guess}
l = Chord
M = number of points used in the quadrature formula of Hadamard's integrals
m = unknown function, doublet distribution
m_a = doublet distribution (chord direction)
m_{guess} = solution of the Euler–Lagrange equation corresponding to λ_{guess}
m_1, m_2 = unknown functions, doublet distributions
m_{1_0}, m_{1_1} = boundary values of m_1
m_{1opt}, m_{2opt} = candidate functions that minimize J, optimal doublet distributions
m_{2_0}, m_{2_1} = boundary values of m_2
$\bar{m}$ = amplitude of the elliptical doublet distribution
P_j = Legendre polynomial of order j
P_N = legendre polynomial of order N
p = pressure
p_∞ = freestream pressure
Q_j = Cauchy integral used in the calculation of w_i^I
s = nondimensional coordinate
s_i = ith node used in the numerical integration of Hadamard's integrals
t = time, nondimensional coordinate
t_l = lth zero of $P_N(t)$, collocation point
u_n = normalwash
V_∞ = freestream velocity
w_i^I = ith weight used in the numerical integration of Hadamard's integrals
x, y, z = coordinate system
x_d, y_d, z_d = coordinates of the point in which the doublet is positioned
$^R\bar{Y}$ = symmetric regular kernel
$^S\bar{Y}$ = symmetric singular kernel
α = twist distribution
α_i = induced angle of attack
Γ = circulation
γ = ratio of the specific heat coefficients for unit mass (1.4 for air)
$\delta_1, \delta_2, \delta_3$ = variation functions
λ = Lagrange multiplier
λ_{guess} = arbitrarily chosen Lagrange multiplier
ρ_∞ = freestream density (constant in all field)
σ = auxiliary variable
Ψ = acceleration potential, small perturbation acceleration potential
ϕ = small perturbation velocity potential
$2b_w$ = wing span
$⨍$ = Hadamard's finite-part integral

Introduction

METHODS for induced-drag prediction and minimization have been pursued since the early days of aviation.[1,2] Reviews of procedures for induced-drag prediction can be found in the literature.[3–5] To calculate the induced drag generated by a lifting surface, it is required[4] that all, or at least a portion, of the velocity field has to be determined in the vicinity of the wing. Linear potential flow methods generally solve for the velocity over only a small part of the flowfield and can, thus, lead to significant computational savings.

Such linear methods can be of the lifting-line theory type.[4,6–11] Lifting surface theories and solution methods such as the vortex-lattice method[4,6,12–23] account for chordwise as well as spanwise effects on thin wings.

Panel methods[24,25] can account for wing thickness and for volume distributions. It is not straightforward, however, to calculate induced drag by integration of drag forces on individual panels in panel and lifting surfaces because the result can be sensitive to discretization, and, thus, both surface integration and Trefftz-plane integration can be used.

Optimal lift distributions for minimum drag on straight high-aspect-ratio wings were already obtained in the early years of the 20th century, and interest in induced-drag minimization kept place with the evolution over the years of more complex wing configurations.[26] With the growing availability of digital computers and math-programming algorithms, first lifting surface/math-programming optimum wing designs for minimum induced drag were reported in the 1960s and early 1970s. Development of math-programming-based wing design for induced drag minimization continued in the 1980s and 1990s, and the technology was applied to emerging unconventional wing configurations, such as the box wing and C wing.[3] Some of the main advantages of the math-programming induced-drag-minimization methods are that they are efficient and can be applied to general configurations subject to constraints of various types. The early analytical induced-drag-minimization methods were applicable only to simple configurations. In this paper a new theoretical approach for induced-drag minimization that can tackle planforms of quite general form and can be applied to nonconventional wing configurations is presented. The method is based on a variational approach and leads to a set of equations for the optimum solution directly. Under the hypotheses of steady, incompressible, and inviscid flow, the induced drag is minimized considering the wake rigid and aligned with the freestream velocity. (The wake can also be modeled as deformed wake).[27–29]

The new method is not intended to replace math-programming-based induced-drag minimization techniques. It complements such methods by shedding light on some of the analytical and numerical issues involved and can provide benchmark test cases for the verification of accuracy and convergence characteristics of other minimization methods.

The paper is organized as follows: the Euler–Lagrange integral equation involving Hadamard finite-part integrals is derived. A numerical solution technique for such an equation is presented. Hadamard integrals appear in the expressions of the induced drag, and their accurate numerical evaluation is required in any direct minimum induced-drag solution using variational calculus based optimality criteria. Thus, a quadrature formula for the Hadamard finite-part integral is introduced. Finally, the present minimization procedure is applied to the biplane case as a demonstration, and results are presented and discussed.

The power of the proposed technique is not limited to planar wings. Important three-dimensional wing configurations can be addressed by the method. The present paper, however, focuses on the presentation of the technique and its demonstration using biplanes only. Applications to more complex configurations will be presented in a subsequent paper.

Mathematical Preliminaries

Euler–Lagrange Equation Involving Hadamard Finite-Part Integrals

Presented here is an extension of the well known Euler–Lagrange equation[30–32] in a particular case, where the integral has to be interpreted in the Hadamard[33–35] finite-part sense. A particular functional is presented here (later it will represent the induced drag in a biplane):

$$J = C_1 \int_{-b_w}^{+b_w} m_1(y_d) \fint_{-b_w}^{+b_w} m_1(y)\, {}^S\bar{Y}(y, y_d)\, \mathrm{d}y\, \mathrm{d}y_d$$

$$+ C_1 \int_{-b_w}^{+b_w} m_1(y_d) \int_{-b_w}^{+b_w} m_2(y)\, {}^R\bar{Y}(y, y_d)\, \mathrm{d}y\, \mathrm{d}y_d$$

$$+ C_1 \int_{-b_w}^{+b_w} m_2(y_d) \fint_{-b_w}^{+b_w} m_2(y)\, {}^S\bar{Y}(y, y_d)\, \mathrm{d}y\, \mathrm{d}y_d$$

$$+ C_1 \int_{-b_w}^{+b_w} m_2(y_d) \int_{-b_w}^{+b_w} m_1(y)\, {}^R\bar{Y}(y, y_d)\, \mathrm{d}y\, \mathrm{d}y_d \tag{1}$$

where ${}^S\bar{Y}(y, y_d)$ is a *singular* kernel of order 2 [in the case of the biplane ${}^S\bar{Y}(y, y_d) = 1/(y - y_d)^2$; in a generic wing system this function is more complex, but the singularity is still of order 2 (Refs. 32 and 36)]. The kernel is also a *symmetric* function in y and y_d: if the variables y and y_d are switched, the kernel does not change: ${}^S\bar{Y}(y, y_d) = {}^S\bar{Y}(y_d, y)$. ${}^R\bar{Y}(y, y_d)$ is a regular and symmetric function: ${}^R\bar{Y}(y, y_d) = {}^R\bar{Y}(y_d, y)$. Notice that the external integrals of the functional *should* be Hadamard's integrals as well. However, in this paper the doublet (or circulation) distribution will be zero at the tips of the wings. Therefore, the singularity is always internal, and, thus, considering that the order of the singularity is 2, the external integrals are defined as standard integrals.

Suppose that the goal is to find the functions m_1 and m_2 that minimize J. Consider, also, a *constraint* of the following type (later the constraint will be represented by the total lifting force):

$$\bar{C} = C_2 \int_{-b_w}^{+b_w} m_1(y_d) g(y_d)\, \mathrm{d}y_d + C_2 \int_{-b_w}^{+b_w} m_2(y_d) g(y_d)\, \mathrm{d}y_d \tag{2}$$

where $g(y_d)$ is a known function. Later the functions m_1 and m_2 will represent the doublet distributions over the wings. The functions m_1 and m_2 have to satisfy the following conditions:

$$m_1(-b_w) = m_{1_0} \qquad m_1(+b_w) = m_{1_1}$$

$$m_2(-b_w) = m_{2_0} \qquad m_2(+b_w) = m_{2_1} \tag{3}$$

In the case of the biplane, $m_{1_0} = m_{1_1} = m_{2_0} = m_{2_1} = 0$. Consider now two variation functions δ_1 and δ_2 that satisfy the conditions

$$\delta_1(-b_w) = \delta_1(+b_w) = 0, \qquad \delta_2(-b_w) = \delta_2(+b_w) = 0 \tag{4}$$

With these variation functions, a solution for the problem can be found using the following relations (the subscript opt indicates the optimal condition: J is minimized):

$$m_1(\cdot) = m_{1\mathrm{opt}}(\cdot) + \sigma \delta_1(\cdot), \qquad m_2(\cdot) = m_{2\mathrm{opt}}(\cdot) + \sigma \delta_2(\cdot)$$

$$\sigma \in (-1, 1) \tag{5}$$

where σ is an auxiliary variable. Notice that in Eq. (5) m_1 and m_2 satisfy the boundary conditions (3), if

$$m_{1\,\mathrm{opt}}(-b_w) = m_{1_0}, \qquad m_{1\,\mathrm{opt}}(+b_w) = m_{1_1}$$

$$m_{2\,\mathrm{opt}}(-b_w) = m_{2_0}, \qquad m_{2\,\mathrm{opt}}(+b_w) = m_{2_1} \tag{6}$$

Notice, also, that $m_{1\,\mathrm{opt}}$ and $m_{2\,\mathrm{opt}}$ are the candidate functions to minimize J. To apply the Lagrange multiplier method for optimization,

constraint (2) has to be manipulated. It can be written as

$$c(y_d) = C_2 \int_{-b_w}^{y_d} m_1(\bar{y})g(\bar{y})\,\mathrm{d}\bar{y} + C_2 \int_{-b_w}^{y_d} m_2(\bar{y})g(\bar{y})\,\mathrm{d}\bar{y}$$

$$\Rightarrow c'(y_d) - C_2 m_1(y_d)g(y_d) - C_2 m_2(y_d)g(y_d) = 0 \qquad (7)$$

where

$$c(+b_w) = \bar{C}, \qquad c(-b_w) = 0 \qquad (8)$$

As can be seen,[32] in order to apply the Lagrange multiplier method the following steps must be taken:

1) Step 1 is substitution of Eq. (5) into the expression representing the functional J [Eq. (1)] and calculation of the derivative with respect to σ. The derivative has to be evaluated for $\sigma = 0$.

2) Step 2 is substitution of $c(\cdot) = c(\cdot)_{\mathrm{opt}} + \sigma\delta_3(\cdot)$ and Eq. (5) into Eq. (7). Notice that $\delta_3(+b_w) = \delta_3(-b_w) = 0$, $c_{\mathrm{opt}}(+b_w) = \bar{C}$, and $c_{\mathrm{opt}}(-b_w) = 0$. After the substitution, the derivative with respect to σ has to be calculated and evaluated for $\sigma = 0$.

Following these steps (details in Appendix A), the Euler–Lagrange equations can be written as

$$+2C_1 \!\!\!\!\fint_{-b_w}^{+b_w} m_{1\mathrm{opt}}(y)^S \bar{Y}(y_d, y)\,\mathrm{d}y$$

$$+2C_1 \int_{-b_w}^{+b_w} m_{2\mathrm{opt}}(y)^R \bar{Y}(y_d, y)\,\mathrm{d}y - C_2\lambda g(y_d) = 0 \qquad (9)$$

$$+2C_1 \!\!\!\!\fint_{-b_w}^{+b_w} m_{2\mathrm{opt}}(y)^S \bar{Y}(y_d, y)\,\mathrm{d}y$$

$$+2C_1 \int_{-b_w}^{+b_w} m_{1\mathrm{opt}}(y)^R \bar{Y}(y_d, y)\,\mathrm{d}y - C_2\lambda g(y_d) = 0 \qquad (10)$$

Equations (9) and (10) represent a system of Euler–Lagrange equations. (Notice that in usual variational problems differential equations are found; in this particular problem, the system is a system of integral equations.)

The constraint for the functions $m_{1\,\mathrm{opt}}$ and $m_{2\,\mathrm{opt}}$ [see Eq. (2)] has to be satisfied as well:

$$\bar{C} = C_2 \int_{-b_w}^{+b_w} m_{1\,\mathrm{opt}}(y_d)g(y_d)\,\mathrm{d}y_d + C_2 \int_{-b_w}^{+b_w} m_{2\,\mathrm{opt}}(y_d)g(y_d)\,\mathrm{d}y_d$$

$$\tag{11}$$

Several important observations can be made. First of all, if other wing systems are analyzed the number of Euler–Lagrange equations can be different. For example, in a rectangular box wing[37] the equations that have to be satisfied are four Euler–Lagrange equations (in the unknown distributions over the horizontal wings and the vertical joints) and the constraint equation (the total lift imposed). Moreover, the distribution, for example, over the upper wing is not zero at the endpoints of the integrals. Therefore, the Hadamard integrals have the singularity not included in the integration domain. This fact does not allow, a priori, the possibility to change the variables (in order to solve the integrals numerically) as in the standard integrals. However, the changing of the variables is allowed if a few extra terms are added.[34] The quadrature formula for the Hadamard integrals is also different than the quadrature formula used when the singularity is internal in the integration domain. In addition, the external integrals that appear in the definition of J (the induced drag expression) have to be defined as Hadamard integrals as well.

Considering these observations, the extension to a general wing system is possible, but particular care has to be devoted to the Hadamard integrals.[34] The author has applied the present minimization procedure to other wing geometries (nonplanar and closed-wing systems). The results will be shown in subsequent papers.

Minimum Induced-Drag Problem—Demonstration Using the Biplane Configuration

In some publications, it is said that the minimum induced drag in a biplane is obtained when the distribution of each wing is el-
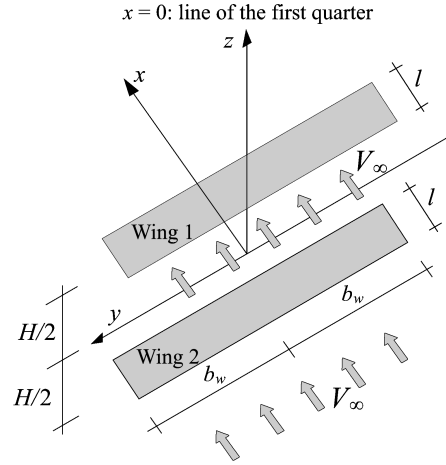

Fig. 1   Biplane: geometry and notations.

liptical and when the wings have the same load distribution. This statement is false. The misunderstanding is from an article,[38] where Prandtl assumed the elliptical distribution for each wing in a biplane and obtained that, under this condition, the best biplane had wings with the same wing span. But Prandtl never stated that the elliptical distribution is the optimal distribution for any biplane. It will be demonstrated that the elliptical circulation distribution is the optimum *only* if the distance between the two wings is either near zero or infinity.

Consider a biplane (see Fig. 1; even if the wings have sweep angles, the biplane depicted in the figure is useful because Munk's stagger theorem[39] can be applied) with wing span $2b_w$ and distance between the wings H. The upper wing (here called wing 1) is positioned at $z = z_1 = +H/2$, while the lower wing (here called wing 2) is positioned at $z = z_2 = -H/2$ in the reference system shown in Fig. 1.

Direct Problem: Weissinger's Approach

Weissinger's lifting-line theory can be used to describe the wings. If the small perturbation acceleration potential[40] is used, the writing of the integral equations (as will be seen, in this case there are two integral equations containing the unknown doublet distributions on the wings 1 and 2) can be accomplished using the procedures shown in the following steps:

1) Step 1: The lift distribution over the wings is modeled using doublet lines along the span. Then, the small perturbation acceleration potential of the doublet distribution m_1 and m_2 over the wings is written.

2) Step 2: The small perturbation velocity potential is obtained by integration of the small perturbation acceleration potential. This operation is necessary because the wall tangency condition (WTC) is written using the components of the velocity, which can be obtained by derivation of the small perturbation velocity potential.

3) Step 3: The WTC is imposed using Weissinger's[8,9] approach.

These operations are defined as direct problem because they allow calculation of the lift distribution over the wings once the twist distribution is assigned.

Small Perturbation Acceleration Potential

Consider wing 1. The generic expression for the small perturbation acceleration potential of a doublet $m_1(y_d)\,\mathrm{d}y_d$ positioned at point $P(x_d, y_d, z_d)$ is

$$\mathrm{d}\Psi_1(x, y, z) =$$

$$-\frac{m_1(y_d)\,\mathrm{d}y_d}{4\pi} \frac{n_{dx}(x - x_d) + n_{dy}(y - y_d) + n_{dz}(z - z_d)}{\left[(x - x_d)^2 + (y - y_d)^2 + (z - z_d)^2\right]^{\frac{3}{2}}} \qquad (12)$$

where n_{dx}, n_{dy}, and n_{dz} are the components of the unit vector, which defines the axis of the doublet $m_1(y_d)\,\mathrm{d}y_d$. Now, choosing the doublet axis to be directed along $+z$ (the opposite choice is equivalent;

however, in some equations the sign has to be changed), it can be deduced that $n_{dx} = n_{dy} = 0$ and $n_{dz} = 1$. Substituting into Eq. (12) and remembering that $z_d = z_1 = +H/2$ and integrating along the span of wing 1:

$$\Psi_1(x, y, z) = -\int_{-b_w}^{+b_w} \frac{m_1(y_d)}{4\pi} \frac{(z - H/2)}{\left[x^2 + (y - y_d)^2 + (z - H/2)^2\right]^{\frac{3}{2}}} \, dy_d$$

(13)

$\Psi_1(x, y, z)$ is the small perturbation acceleration potential obtained by adding all contributions of all doublets on wing 1.

The same operations can be repeated for wing 2:

$$\Psi_2(x, y, z) = -\int_{-b_w}^{+b_w} \frac{m_2(y_d)}{4\pi} \frac{(z + H/2)}{\left[x^2 + (y - y_d)^2 + (z + H/2)^2\right]^{\frac{3}{2}}} \, dy_d$$

(14)

The theory that is being developed is linear. Therefore, the superimposition of the contributions is possible. Thus, the small perturbation acceleration potential of the biplane is obtained by adding Eqs. (13) and (14)

$$\Psi(x, y, z) = \Psi_1(x, y, z) + \Psi_2(x, y, z) \quad (15)$$

Small Perturbation Velocity Potential

To impose the boundary conditions, the small perturbation velocity potential has to be written by integrating the expression of the small perturbation acceleration potential:

$$\phi(x, y, z) = \phi_1 + \phi_2$$

$$= \frac{1}{V_\infty} \int_{-\infty}^{x} \Psi_1(\tau, y, z) \, d\tau + \frac{1}{V_\infty} \int_{-\infty}^{x} \Psi_2(\tau, y, z) \, d\tau \quad (16)$$

where ϕ_1 and ϕ_2 are the contributes of the wings 1 and 2, respectively. Calculating the integrals, the explicit form of the small perturbation velocity potential can be written as

$$\phi_1 = -\frac{1}{4\pi V_\infty} \int_{-b_w}^{+b_w} \frac{m_1(y_d)(z - H/2)}{(y - y_d)^2 + (z - H/2)^2}$$

$$\times \left[\frac{x}{\sqrt{x^2 + (y - y_d)^2 + (z - H/2)^2}} + 1\right] dy_d \quad (17)$$

$$\phi_2 = -\frac{1}{4\pi V_\infty} \int_{-b_w}^{+b_w} \frac{m_2(y_d)(z + H/2)}{(y - y_d)^2 + (z + H/2)^2}$$

$$\times \left[\frac{x}{\sqrt{x^2 + (y - y_d)^2 + (z + H/2)^2}} + 1\right] dy_d \quad (18)$$

WTC Imposition Using Weissinger's Approach

The WTC has to be imposed on both wings. Thus,

$$-\alpha_1(y, z_1) = \frac{1}{V_\infty} \left[\frac{\partial \phi}{\partial z}\right]_{z = z_1, \, x = x_{\text{WTC}}}$$

$$-\alpha_2(y, z_2) = \frac{1}{V_\infty} \left[\frac{\partial \phi}{\partial z}\right]_{z = z_2, \, x = x_{\text{WTC}}} \quad (19)$$

where $x_{\text{WTC}} = l/2$, $z_1 = +H/2$ and $z_2 = -H/2$. Notice that the doublet distributions are positioned at $x = 0$ (first quarter line), but the boundary conditions are imposed at $x_{\text{WTC}} = l/2$.

There is no requirement that imposes $m_1(y) = m_2(y)$ because the wings can have different aerodynamic properties (for example, the twist distribution); hence, in general, $m_1(y) \neq m_2(y)$. The system of integral equations [see Eq. (19)] can be used to solve the direct problem: when the velocity V_∞ and the twist distributions $\alpha(y, z_1)$ and $\alpha(y, z_2)$ are known, the unknown doublet distributions $m_1(y)$ and $m_2(y)$ over the wings 1 and 2 can be calculated, and from those quantities the calculation of the lifting force and induced drag is straightforward. The direct problem[41] will not be solved here.

Normalwash

The normalwash u_n is involved in the induced drag formula, as it will be shown in the next section. Then u_n follows from the definition of the small perturbation velocity potential. Consider wing 1. The induced velocity has the expression

$$u_{n1} = \left[\frac{\partial \phi}{\partial z}\right]_{z = z_1, x = 0} = \left[\frac{\partial \phi_1}{\partial z}\right]_{z = z_1, x = 0} + \left[\frac{\partial \phi_2}{\partial z}\right]_{z = z_1, x = 0} \quad (20)$$

Using Eqs. (17) and (18), and remembering that $z_1 = +H/2$, Eq. (20) can give the normalwash for wing 1:

$$u_{n1}(y) = -\frac{1}{4\pi V_\infty} \fint_{-b_w}^{+b_w} \frac{m_1(y_d)}{(y - y_d)^2} \, dy_d$$

$$- \frac{1}{4\pi V_\infty} \int_{-b_w}^{+b_w} m_2(y_d) \frac{(y - y_d)^2 - H^2}{\left[(y - y_d)^2 + H^2\right]^2} \, dy_d \quad (21)$$

Similarly for wing 2, it can be shown that

$$u_{n2}(y) = -\frac{1}{4\pi V_\infty} \fint_{-b_w}^{+b_w} \frac{m_2(y_d)}{(y - y_d)^2} \, dy_d$$

$$- \frac{1}{4\pi V_\infty} \int_{-b_w}^{+b_w} m_1(y_d) \frac{(y - y_d)^2 - H^2}{\left[(y - y_d)^2 + H^2\right]^2} \, dy_d \quad (22)$$

Aerodynamic Force per Unit of Length of Wing Span

The definition of acceleration potential is

$$\Psi = -\int \frac{dp}{\rho} - G(t) \quad (23)$$

where $G(t)$ is a function of time t and furnishes the value of Ψ at the start of the integration domain. In the isentropic case, it is not difficult to show that

$$\Psi = [\gamma/(\gamma - 1)]\left(p_\infty^{1/\gamma} / \rho_\infty\right)\left[p_\infty^{(\gamma - 1)/\gamma} - p^{(\gamma - 1)/\gamma}\right] \quad (24)$$

Using the hypothesis of small perturbations, the pressure can be expanded from the value p_∞ by using the following Taylor series:

$$p^{(\gamma - 1)/\gamma} = p_\infty^{(\gamma - 1)/\gamma}\{1 + [(\gamma - 1)/\gamma](p/p_\infty - 1)\} \quad (25)$$

Substituting Eq. (25) into Eq. (24), the small perturbation acceleration potential becomes

$$\Psi = (p_\infty - p)/\rho_\infty \quad (26)$$

which shows that the small perturbation acceleration potential is directly related to the pressure. To show how to calculate the aerodynamic force using the doublet distributions, consider an airfoil (two-dimensional case). The x direction is the direction of the chord and the freestream velocity V_∞; the z direction is the direction of the lifting force. The small perturbation hypothesis signifies that the airfoil can be studied using a distribution of doublets $m_a(x)$ along the chord of the airfoil. Suppose that the axes of the doublets are directed along $+z$. Notice that the airfoil can be thought as a section in $y = y_d$ of a wing in the $x - y$ plane. The $m_a(x)$ should not be confused with $m(y_d)$: $m_a(x)$ is the distribution of doublets in the chord direction of the airfoil positioned at $y = y_d$; $m(y_d)$ is its integral:

$$m(y_d) = \int_{-\frac{1}{4}l}^{+\frac{3}{4}l} m_a(x) \, dx \quad (27)$$

The small perturbation acceleration potential of the doublets $m_a(x)$ is (notice that this is a two-dimensional case)

$$\Psi(x, z) = -\frac{1}{2\pi} \int_{-\frac{1}{4}l}^{+\frac{3}{4}l} m_a(\xi) \frac{z}{(x - \xi)^2 + z^2} \, d\xi \quad (28)$$

From Eq. (28), it follows that

$$\Psi(x, 0^{\pm}) = \mp m_a(x)/2 \tag{29}$$

Using the relation between the small perturbation acceleration potential and the pressure [Eq. (26)] and Eq. (29), the aerodynamic force per unit of area F_a is

$$F_a(x) = -\rho_\infty[\Psi(x, 0^-) - \Psi(x, 0^+)]$$

$$= -\rho_\infty[m_a(x)/2 + m_a(x)/2] = -\rho_\infty m_a(x) \tag{30}$$

In Weissinger's approach, all doublets $m_a(x)$ of the generic airfoil positioned at $y = y_d$ are concentrated at the point $x = x_d = 0$ (first quarter), and the WTC is imposed at the point $x_{\text{WTC}} = +\frac{1}{2}l$. Therefore, in the generic airfoil the aerodynamic force (per unit of length of wing span) is obtained as follows:

$$F(y_d) = \int_{-\frac{1}{4}l}^{+\frac{3}{4}l} F_a(x)\,dx = -\rho_\infty \int_{-\frac{1}{4}l}^{+\frac{3}{4}l} m_a(x)\,dx = -\rho_\infty m(y_d) \tag{31}$$

If the doublets are chosen with axes direct along $-z$, the preceding equation has the $+$ sign. Considering what has been proved here, it is not difficult to relate the doublet distribution to the circulation $\Gamma(y_d)$. This can be done by considering the local Kutta–Joukowsky theorem:

$$F(y_d) = \rho_\infty V_\infty \Gamma(y_d) \tag{32}$$

Comparing Eqs. (31) and (32), the relation between the circulation distribution and the doublet distribution is

$$\Gamma(y_d) = -m(y_d)/V_\infty \tag{33}$$

Therefore, when in the next sections the optimal doublet distribution is found, the optimal circulation distribution can be obtained by multiplying the doublet distribution by a constant [see Eq. (33)].

Relation (33) can be also applied in the geometrical derivation[32] of the normalwash. In fact, it is possible to use the circulation distribution over the wings and calculate the induced velocity using Biot–Savart[6] law. Then integrating by parts and recalling that the circulation has to be zero at the tips, the normalwash as a function of the circulation (and not of its derivatives) can be calculated. Finally, using Eq. (33), the normalwash equations can be shown to be coincident with expressions (21) and (22) obtained deriving the velocity potential.

Induced Drag

The goal is to minimize the induced drag. To do that, the mathematical expression of the induced drag has to be formulated in terms of $m_1(y)$ and $m_2(y)$.

Consider the upper wing (wing 1). The axes of the doublets are directed along $+z$. Hence, the aerodynamic force per unit of length is

$$F_1(y_d) = -\rho_\infty m_1(y_d) \tag{34}$$

The induced incidence on the wing 1 is calculated using the normalwash:

$$\alpha_{i1}(y_d) = -[u_{n1}(y_d)]_{x=0}/V_\infty \tag{35}$$

The induced drag per unit of span is $F_1(y_d) \tan[\alpha_{i1}(y_d)]$. Integrating over the wing span and remembering that the formulation is valid for small perturbations (i.e., the trigonometric tangent is approximated with the angle), the induced drag contribute of the wing 1 is

$$D_{i1} = \int_{-b_w}^{+b_w} F(y_d) \tan[\alpha_{i1}(y_d)]\,dy_d \simeq \int_{-b_w}^{+b_w} F_1(y_d)\alpha_{i1}(y_d)\,dy_d \tag{36}$$

Using Eqs. (34) and (35) and the normalwash expression on the wing 1 [Eq. (21)], the contribution on the induced drag of the upper wing is

$$D_{i1} = -\frac{\rho_\infty}{4\pi V_\infty^2} \int_{-b_w}^{+b_w} m_1(y_d) \fint_{-b_w}^{+b_w} \frac{m_1(y)}{(y - y_d)^2}\,dy\,dy_d$$

$$- \frac{\rho_\infty}{4\pi V_\infty^2} \int_{-b_w}^{+b_w} m_1(y_d) \int_{-b_w}^{+b_w} m_2(y) \frac{(y - y_d)^2 - H^2}{\left[(y - y_d)^2 + H^2\right]^2}\,dy\,dy_d \tag{37}$$

Notice that both wings give a contribution on the induced drag. Repeating the same procedure for the wing 2,

$$D_{i2} = -\frac{\rho_\infty}{4\pi V_\infty^2} \int_{-b_w}^{+b_w} m_2(y_d) \fint_{-b_w}^{+b_w} \frac{m_2(y)}{(y - y_d)^2}\,dy\,dy_d$$

$$- \frac{\rho_\infty}{4\pi V_\infty^2} \int_{-b_w}^{+b_w} m_2(y_d) \int_{-b_w}^{+b_w} m_1(y) \frac{(y - y_d)^2 - H^2}{\left[(y - y_d)^2 + H^2\right]^2}\,dy\,dy_d \tag{38}$$

The total induced drag is the summation of the contributes of wings 1 and 2:

$$D_i = D_{i1} + D_{i2} \tag{39}$$

Total Lifting Force

Recalling the expression of the aerodynamic force [Eq. (34)], the expression for total lifting force can be written as

$$L = L_1 + L_2 = -\rho_\infty \int_{-b_w}^{+b_w} m_1(y_d)\,dy_d - \rho_\infty \int_{-b_w}^{+b_w} m_2(y_d)\,dy_d \tag{40}$$

Derivation of the Euler–Lagrange Equations

The purpose is to minimize the induced drag under the condition of fixed total lifting force and wing span. To achieve this goal, the methods explained in the preceding sections have to be applied. The functional that has to be minimized is represented by Eq. (39); the constraint is represented by the condition of fixed total lifting force $L = \bar{L}$ [see Eq. (40)]. Comparing Eqs. (39), (37), (38), and (40) with Eqs. (1) and (2), it follows that

$$C_1 = -\frac{\rho_\infty}{4\pi V_\infty^2} \qquad C_2 = -\rho_\infty \qquad g(y_d) = 1 \qquad \bar{C} = \bar{L}$$

$$^S\bar{Y} = \frac{1}{(y - y_d)^2} \qquad ^R\bar{Y} = \frac{(y - y_d)^2 - H^2}{\left[(y - y_d)^2 + H^2\right]^2} \tag{41}$$

Therefore, Eqs. (9) and (10) can be written as

$$\fint_{-b_w}^{+b_w} \frac{m_{1\,\text{opt}}(y)}{(y - y_d)^2}\,dy + \int_{-b_w}^{+b_w} m_{2\,\text{opt}}(y) \frac{(y - y_d)^2 - H^2}{\left[(y - y_d)^2 + H^2\right]^2}\,dy$$

$$- \lambda \cdot 2\pi V_\infty^2 = 0 \tag{42}$$

$$\fint_{-b_w}^{+b_w} \frac{m_{2\,\text{opt}}(y)}{(y - y_d)^2}\,dy + \int_{-b_w}^{+b_w} m_{1\,\text{opt}}(y) \frac{(y - y_d)^2 - H^2}{\left[(y - y_d)^2 + H^2\right]^2}\,dy$$

$$- \lambda \cdot 2\pi V_\infty^2 = 0 \tag{43}$$

The following can be observed:

1) One equation is identical to the other if the subscripts 1 and 2 are switched. This implies that, under optimal conditions, the distributions on the wings must be the same: $m_{1\,\text{opt}} = m_{2\,\text{opt}}$.

2) Under optimal condition the induced velocity over the wings must be constant. This can be seen considering the expressions

valid for u_{n1} and u_{n2} [Eqs. (21) and (22)] and comparing them with Eqs. (42) and (43). (Notice that $\lambda \cdot 2\pi V_\infty^2$ is a constant.)

3) Munk's minimum induced drag theorem[39] is satisfied because $u_n = $ const in both wings. Notice that if other optimality conditions are imposed (like the structural weight), then this theorem is no longer valid,[42,43] and the Euler–Lagrange equations are different.

4) Setting $m_{1\,\mathrm{opt}} = m_{2\,\mathrm{opt}} = m_\mathrm{opt}$, the system of Euler–Lagrange equations becomes a single Euler–Lagrange equation in the unknown m_opt. Therefore, from now on only a single Euler–Lagrange equation and the constraint will be considered:

$$\begin{cases} \fint_{-b_w}^{+b_w} \frac{m_\mathrm{opt}(y)}{(y-y_d)^2}\,\mathrm{d}y + \int_{-b_w}^{+b_w} m_\mathrm{opt}(y) \frac{(y-y_d)^2 - H^2}{\left[(y-y_d)^2 + H^2\right]^2}\,\mathrm{d}y \\ \qquad - \lambda \cdot 2\pi V_\infty^2 = 0 \\ \bar{L} = -2\rho_\infty \int_{-b_w}^{+b_w} m_\mathrm{opt}(y)\,\mathrm{d}y \end{cases} \tag{44}$$

The numerical procedure adopted to solve the system (44) is reported in Appendix B. The general case, in which more constraints are applied, is discussed in Appendix B as well. The quadrature formula for the Hadamard integral is reported in Appendix C.

Validation—Optimal Doublet Distribution: $H \to 0$ Case

When $H \to 0$, the equation of the minimum induced drag [see Eqs. (37) and (38)] becomes

$$(D_i)_\mathrm{opt} = -\frac{\rho_\infty}{\pi V_\infty^2}\int_{-b_w}^{+b_w} m_\mathrm{opt}(y_d)\left[\fint_{-b_w}^{+b_w} \frac{m_\mathrm{opt}(y)}{(y-y_d)^2}\,\mathrm{d}y\right]\mathrm{d}y_d \quad (45)$$

The Euler–Lagrange equation and the constraint assume the form

$$\begin{cases} -\frac{1}{\pi V_\infty^2}\fint_{-b_w}^{+b_w} \frac{m_\mathrm{opt}(y)}{(y-y_d)^2}\,\mathrm{d}y + \lambda = 0 \\ \bar{L} = -2\rho_\infty \int_{-b_w}^{+b_w} m_\mathrm{opt}(y)\,\mathrm{d}y \end{cases} \tag{46}$$

It is not difficult to understand that the system is structurally similar to the equivalent system obtained for the classical cantilevered wing (see Appendix D). Therefore, the solution is still an elliptical distribution. (The difference between the two systems is only in some constants.) Using the same procedure reported in Appendix D, it can be concluded that when $H \to 0$ the optimal distribution is elliptical and the induced drag is the same as an optimally loaded classical wing with the same total lift and wing span. In fact, from Eq. (46) and assuming the elliptical distribution

$$m_\mathrm{opt}(y) = \bar{m}\sqrt{1 - y^2/b_w^2} \tag{47}$$

using the relations (see Appendix D for their derivation)

$$\begin{aligned} \fint_{-b_w}^{+b_w} \frac{m_\mathrm{opt}(y)}{(y-y_d)^2}\,\mathrm{d}y &= -\bar{m}\frac{\pi}{b_w} \\ \int_{-b_w}^{+b_w} m_\mathrm{opt}(y)\,\mathrm{d}y &= \bar{m}\frac{b_w\pi}{2} \end{aligned} \tag{48}$$

The system (46) becomes

$$\begin{cases} -\left[1/\left(\pi V_\infty^2\right)\right]\left[-\bar{m}(\pi/b_w)\right] + \lambda = 0 \Rightarrow \lambda = \bar{L}/\left(\rho_\infty \pi b_w^2 V_\infty^2\right) \\ \bar{L} = -2\rho_\infty[\bar{m}(b_w\pi/2)] \Rightarrow \bar{m} = -\bar{L}/(\rho_\infty \pi b_w) \end{cases} \tag{49}$$

Using the second relation of Eqs. (49) and (48), the minimum induced drag [Eq. (45)] becomes

$$(D_i)_\mathrm{opt} = -\frac{\rho_\infty}{\pi V_\infty^2}\left(-\bar{m}\frac{\pi}{b_w}\right)\left(\bar{m}\frac{b_w\pi}{2}\right) = \frac{\rho_\infty \pi}{2V_\infty^2}\bar{m}^2 =$$

$$= \frac{\rho_\infty \pi}{2V_\infty^2}\left(-\frac{\bar{L}}{\rho_\infty \pi b_w}\right)^2 = \frac{\bar{L}^2}{2\pi\rho_\infty b_w^2 V_\infty^2} \tag{50}$$

which demonstrates that the minimum induced drag is the same as the minimum induced drag of a cantileverd wing with the same wing span and total lift (see Appendix D). Notice that it is correct to have the negative sign in the expression of $\bar{m}$ [see Eq. (49)]. The meaning is that the doublets have to have an opposite axis direction with respect to the initial choice (which was $+z$) in order to have the lift directed along $+z$.

Validation—Optimal Doublet Distribution: $H \to \infty$ Case

Calculating the limit $H \to \infty$, the minimum induced-drag expression [compare the following expression with Eq. (45), valid for the case $H \to 0$] becomes

$$(D_i)_\mathrm{opt} = -\frac{\rho_\infty}{2\pi V_\infty^2}\int_{-b_w}^{+b_w} m_\mathrm{opt}(y_d)\left[\fint_{-b_w}^{+b_w} \frac{m_\mathrm{opt}(y)}{(y-y_d)^2}\,\mathrm{d}y\right]\mathrm{d}y_d \tag{51}$$

The system represented by the Euler–Lagrange equation and the constraint is

$$\begin{cases} -\frac{1}{2\pi V_\infty^2}\fint_{-b_w}^{+b_w} \frac{m_\mathrm{opt}(y)}{(y-y_d)^2}\,\mathrm{d}y + \lambda = 0 \\ \bar{L} = -2\rho_\infty \int_{-b_w}^{+b_w} m_\mathrm{opt}(y)\,\mathrm{d}y \end{cases} \tag{52}$$

Again, the solution is represented by an elliptical distribution. In particular, it is possible to find

$$\bar{m} = -\bar{L}/(\rho_\infty \pi b_w), \qquad (D_i)_\mathrm{opt} = \bar{L}^2\big/\left(4\pi\rho_\infty b_w^2 V_\infty^2\right) \tag{53}$$

Comparing Eqs. (50) and (53), it is possible to deduce that $\frac{1}{2}$ the induced drag of an optimally loaded cantilevered wing with the same lift and wing span has been found.

Optimal Doublet Distribution: Finite H Case

Is the optimal distribution elliptical? To answer the question, it is useful to change the variables and manipulate the Euler–Lagrange equation [first relation in Eq. (44)]. Setting $s = y/b_w \Rightarrow y = sb_w$, $t = y_d/b_w \Rightarrow y_d = tb_w$ and $h = H/b_w$, the Euler–Lagrange equation becomes

$$\int_{-1}^{+1} m_\mathrm{opt}(s)\frac{(t-s)^2 - h^2}{[(t-s)^2 + h^2]^2}\,\mathrm{d}s + \fint_{-1}^{+1} \frac{m_\mathrm{opt}(s)}{(t-s)^2}\,\mathrm{d}s$$

$$- \lambda \cdot 2\pi b_w V_\infty^2 = 0 \tag{54}$$

Suppose that the optimal distribution is elliptical. Then, the distribution $(m)_\mathrm{opt}$ should have the expression $(m)_\mathrm{opt}(s) = \bar{m}\sqrt{(1 - s^2)}$. Substituting this expression into Eq. (54), Eq. (54) has to be satisfied. Now consider the Lagrange multiplier: it is constant. The Hadamard finite-part integral is constant as well because the distribution is elliptical (see the demonstration in Appendix D). Therefore, it is evident that Eq. (54) can be satisfied under elliptical distribution only if

$$\int_{-1}^{+1} m_\mathrm{opt}(s)\frac{(t-s)^2 - h^2}{[(t-s)^2 + h^2]^2}\,\mathrm{d}s$$

$$= \int_{-1}^{+1} \bar{m}\sqrt{1 - s^2}\frac{(t-s)^2 - h^2}{[(t-s)^2 + h^2]^2}\,\mathrm{d}s = \mathrm{const} \tag{55}$$

In other words, for a fixed value of the parameter h the integral must not be dependent on the value of the variable t. For example, consider $h = -\bar{m} = 1$. It is easy to see that the integral is not constant with t. For example, using $t = 0.2$ and -0.5 yields different values:

$$-\int_{-1}^{+1} \sqrt{1 - s^2}\frac{(0.2 - s)^2 - 1}{[(0.2 - s)^2 + 1]^2}\,\mathrm{d}s = +0.8869751615$$

$$-\int_{-1}^{+1} \sqrt{1 - s^2}\frac{(-0.5 - s)^2 - 1}{[(-0.5 - s)^2 + 1]^2}\,\mathrm{d}s$$

$$= +0.7188925775 \neq +0.8869751615 \tag{56}$$

Thus, it has been demonstrated that, under optimal condition, the doublet distribution is not elliptical if the distance H between the wings is finite (not zero). This will be further demonstrated in the next section.

Numerical Evaluations

In preceding sections the optimization problem was examined theoretically. Here, a few numerical solutions to the optimization problem will be analyzed. All results are obtained using the techniques shown in preceding sections. In particular, the Euler–Lagrange equation is solved using the collocation method and guessing the initial value of the Lagrange multiplier λ (see Appendix B).

Consider a biplane with the following data (the reference surface for the nondimensional coefficients of lift and induced drag is $S = 4b_w l$): $C_L = 1.0$ and $b_w/l = 12$ (l is the chord). The effect of the parameter H/l is now discussed. The following cases are analyzed:

1) Case 1 is the $H \to 0$ case. It is studied considering $H/l = 0.1 \times 10^{-3}$.

2) Case 2 is the $H \to \infty$ case. It is studied considering $H/l = 0.1 \times 10^{+3}$.

3) Case 3 is the finite H case. It is studied considering $H/l = 6$.

Recall that, in the biplane with two wings of the same span $2b_w$, the optimal distribution is the same over the two wings. Therefore, it is not important to specify the wing in which the distribution is considered. In all of the examined cases, $m(y) = -\Gamma(y)V_\infty$, where the negative sign is a consequence of the chosen positive direction of the doublets and where $\Gamma(y)$ is the circulation. The numerical drag minimization solution using the technique presented here matches the well-known elliptical load distribution solutions for single wings
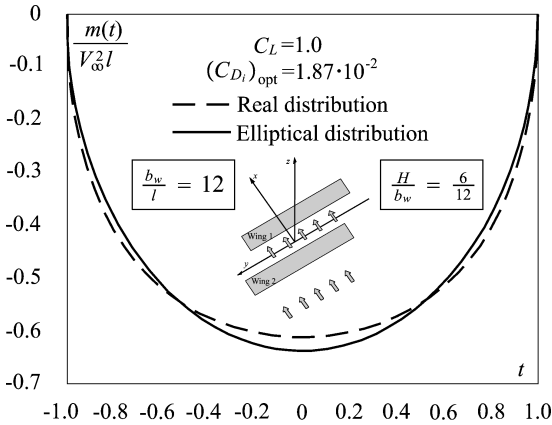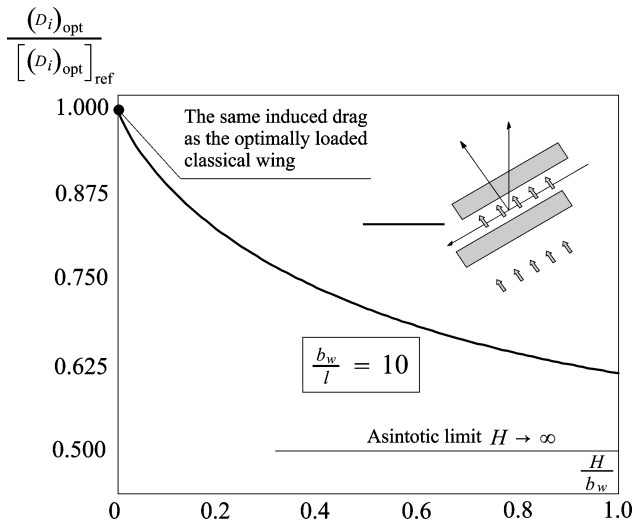
Table 1 Optimal induced-drag coefficient vs H/b_w

H/b_w	$100 \cdot (C_{D_i})_{opt}$	H/b_w	$100 \cdot (C_{D_i})_{opt}$
0.00	3.18	0.50	2.25
0.01	3.11	0.55	2.21
0.05	2.95	0.60	2.17
0.10	2.81	0.65	2.13
0.15	2.70	0.70	2.10
0.20	2.61	0.75	2.07
0.25	2.53	0.80	2.04
0.30	2.46	0.85	2.02
0.35	2.40	0.90	2.00
0.40	2.34	0.95	1.97
0.45	2.29	1.00	1.95

when in the biplane case the distance between the wings is taken to the limit of $H \to 0$ and also $H \to \infty$. In the case of $H \to \infty$, the induced-drag coefficient is found to be $\frac{1}{2}$ of its value when $H \to 0$ (assuming the same total coefficient of lift in the two cases).

The optimal nondimensional doublet distribution along a wing is plotted against the elliptical distribution for the case of finite H in Fig. 2. In the numerical solution of the Euler–Lagrange equation, 20 collocation points are used. It is clear that the preceding theoretical considerations are correct: in the general case, the optimal doublet (or circulation) distribution along a wing in a biplane is not elliptical. The optimal distribution is elliptical only when the distance between the wings is near zero or infinity. The behavior of the induced drag is more clear when Fig. 3 and Table 1 are analyzed. (For those analyses, $b_w/l = 10$ and $C_L = 1.0$ have been considered.) In particular, the optimal induced drag starts from the same value as the classical wing, and it decreases as H increases. This is a general result for nonplanar wings.[3,44]

Conclusions

A general variational induced-drag minimization procedure has been presented and used to study biplane wings. Optimality conditions for lift distributions that minimize induced drag and are subject to constant lift constraints are obtained in closed form, and the results can serve as test cases for the validation of other induced-drag minimization techniques. It has been demonstrated that, for a biplane under optimum conditions, the wings have the same doublet distribution, which in general is not elliptical. The methods exposed here can be used to study more general nonplanar lifting configurations such as arcs or closed-wing systems. The present paper lays the theoretical/numerical foundation of the new technique. Applications to arc wings and closed wings will be presented in subsequent papers.

Fig. 2 Optimal doublet distribution for finite H. Comparison with the elliptical distribution.

Fig. 3 Optimal induced-drag coefficient ratio vs H/b_w.

Appendix A: Derivation of the Euler–Lagrange Equations

The first step is now performed.

Substituting Eq. (5) into the functional J, the resulting expression is

$$J[m_{1\,opt}(\cdot) + \sigma\delta_1(\cdot), m_{2\,opt}(\cdot) + \sigma\delta_2(\cdot)]$$

$$= C_1 \int_{-b_w}^{+b_w} [m_{1\,opt}(y_d) + \sigma\delta_1(y_d)]$$

$$\times \oint_{-b_w}^{+b_w} [m_{1\,opt}(y) + \sigma\delta_1(y)]^S \bar{Y} \, dy \, dy_d$$

$$+ C_1 \int_{-b_w}^{+b_w} [m_{1\,opt}(y_d) + \sigma\delta_1(y_d)]$$

$$\times \int_{-b_w}^{+b_w} [m_{2\,opt}(y) + \sigma\delta_2(y)]^R \bar{Y} \, dy \, dy_d$$

$$+ C_1 \int_{-b_w}^{+b_w} [m_{2\,\text{opt}}(y_d) + \sigma \delta_2(y_d)]$$

$$\times \fint_{-b_w}^{+b_w} [m_{2\,\text{opt}}(y) + \sigma \delta_2(y)]^S \bar{Y} \, dy \, dy_d$$

$$+ C_1 \int_{-b_w}^{+b_w} [m_{2\,\text{opt}}(y_d) + \sigma \delta_2(y_d)]$$

$$\times \int_{-b_w}^{+b_w} [m_{1\,\text{opt}}(y) + \sigma \delta_1(y)]^R \bar{Y} \, dy \, dy_d \qquad \text{(A1)}$$

From this expression, the derivative with respect to σ can be calculated:

$$\frac{dJ}{d\sigma} = C_1 \int_{-b_w}^{+b_w} \delta_1(y_d) \fint_{-b_w}^{+b_w} [m_{1\,\text{opt}}(y) + \sigma \delta_1(y)]^S \bar{Y} \, dy \, dy_d$$

$$+ C_1 \int_{-b_w}^{+b_w} [m_{1\,\text{opt}}(y_d) + \sigma \delta_1(y_d)] \fint_{-b_w}^{+b_w} \delta_1(y)^S \bar{Y} \, dy \, dy_d$$

$$+ C_1 \int_{-b_w}^{+b_w} \delta_1(y_d) \int_{-b_w}^{+b_w} [m_{2\,\text{opt}}(y) + \sigma \delta_2(y)]^R \bar{Y} \, dy \, dy_d$$

$$+ C_1 \int_{-b_w}^{+b_w} [m_{1\,\text{opt}}(y_d) + \sigma \delta_1(y_d)] \int_{-b_w}^{+b_w} \delta_2(y)^R \bar{Y} \, dy \, dy_d$$

$$+ C_1 \int_{-b_w}^{+b_w} \delta_2(y_d) \fint_{-b_w}^{+b_w} [m_{2\,\text{opt}}(y) + \sigma \delta_2(y)]^S \bar{Y} \, dy \, dy_d$$

$$+ C_1 \int_{-b_w}^{+b_w} [m_{2\,\text{opt}}(y_d) + \sigma \delta_2(y_d)] \fint_{-b_w}^{+b_w} \delta_2(y)^S \bar{Y} \, dy \, dy_d$$

$$+ C_1 \int_{-b_w}^{+b_w} \delta_2(y_d) \int_{-b_w}^{+b_w} [m_{1\,\text{opt}}(y) + \sigma \delta_1(y)]^R \bar{Y} \, dy \, dy_d$$

$$+ C_1 \int_{-b_w}^{+b_w} [m_{2\,\text{opt}}(y_d) + \sigma \delta_2(y_d)] \int_{-b_w}^{+b_w} \delta_1(y)^R \bar{Y} \, dy \, dy_d \qquad \text{(A2)}$$

The derivative, calculated for $\sigma = 0$, is

$$\left[\frac{dJ}{d\sigma} \right]_{\sigma=0} = C_1 \int_{-b_w}^{+b_w} \delta_1(y_d) \fint_{-b_w}^{+b_w} m_{1\,\text{opt}}(y)^S \bar{Y} \, dy \, dy_d$$

$$+ C_1 \int_{-b_w}^{+b_w} m_{1\,\text{opt}}(y_d) \fint_{-b_w}^{+b_w} \delta_1(y)^S \bar{Y} \, dy \, dy_d$$

$$+ C_1 \int_{-b_w}^{+b_w} \delta_1(y_d) \int_{-b_w}^{+b_w} m_{2\,\text{opt}}(y)^R \bar{Y} \, dy \, dy_d$$

$$+ C_1 \int_{-b_w}^{+b_w} m_{1\,\text{opt}}(y_d) \int_{-b_w}^{+b_w} \delta_2(y)^R \bar{Y} \, dy \, dy_d$$

$$+ C_1 \int_{-b_w}^{+b_w} \delta_2(y_d) \fint_{-b_w}^{+b_w} m_{2\,\text{opt}}(y)^S \bar{Y} \, dy \, dy_d$$

$$+ C_1 \int_{-b_w}^{+b_w} m_{2\,\text{opt}}(y_d) \fint_{-b_w}^{+b_w} \delta_2(y)^S \bar{Y} \, dy \, dy_d$$

$$+ C_1 \int_{-b_w}^{+b_w} \delta_2(y_d) \int_{-b_w}^{+b_w} m_{1\,\text{opt}}(y)^R \bar{Y} \, dy \, dy_d$$

$$+ C_1 \int_{-b_w}^{+b_w} m_{2\,\text{opt}}(y_d) \int_{-b_w}^{+b_w} \delta_1(y)^R \bar{Y} \, dy \, dy_d \qquad \text{(A3)}$$

Switching y_d and y, using the symmetry of the functions $^R\bar{Y}$, and $^S\bar{Y}$ and exchanging the order of integration (for the integrals defined in the Hadamard finite-part sense this operation can be proven to be correct[32]), Eq. (A3) becomes

$$\left[\frac{dJ}{d\sigma} \right]_{\sigma=0} = 2C_1 \int_{-b_w}^{+b_w} \delta_1(y_d) \fint_{-b_w}^{+b_w} m_{1\,\text{opt}}(y)^S \bar{Y} \, dy \, dy_d$$

$$+ 2C_1 \int_{-b_w}^{+b_w} \delta_1(y_d) \int_{-b_w}^{+b_w} m_{2\,\text{opt}}(y)^R \bar{Y} \, dy \, dy_d$$

$$+ 2C_1 \int_{-b_w}^{+b_w} \delta_2(y_d) \fint_{-b_w}^{+b_w} m_{2\,\text{opt}}(y)^S \bar{Y} \, dy \, dy_d$$

$$+ 2C_1 \int_{-b_w}^{+b_w} \delta_2(y_d) \int_{-b_w}^{+b_w} m_{1\,\text{opt}}(y)^R \bar{Y} \, dy \, dy_d \qquad \text{(A4)}$$

Step 2 is now performed.

Calculating the derivative for the constraint written in Eq. (7), it is possible to write

$$\left[\frac{d}{d\sigma} \{ [c_{\text{opt}}(y_d) + \sigma \delta_3(y_d)]' \right.$$

$$- C_2 [m_{1\,\text{opt}}(y_d) + \sigma \delta_1(y_d)] g(y_d)$$

$$\left. - C_2 [m_{2\,\text{opt}}(y_d) + \sigma \delta_2(y_d)] g(y_d) \} \right]_{\sigma=0}$$

$$= \delta_3'(y_d) - C_2 \delta_1(y_d) g(y_d) - C_2 \delta_2(y_d) g(y_d) = 0 \qquad \text{(A5)}$$

Multiplying this expression by $\lambda(y_d)$, integrating by parts the term that contains the derivative of δ_3 $[\delta_3(+b_w) = \delta_3(-b_w) = 0]$ and adding the result to Eq. (A4) yields the following expression:

$$2C_1 \int_{-b_w}^{+b_w} \delta_1(y_d) \fint_{-b_w}^{+b_w} m_{1\,\text{opt}}(y)^S \bar{Y} \, dy \, dy_d$$

$$+ 2C_1 \int_{-b_w}^{+b_w} \delta_1(y_d) \int_{-b_w}^{+b_w} m_{2\,\text{opt}}(y)^R \bar{Y} \, dy \, dy_d$$

$$+ 2C_1 \int_{-b_w}^{+b_w} \delta_2(y_d) \fint_{-b_w}^{+b_w} m_{2\,\text{opt}}(y)^S \bar{Y} \, dy \, dy_d$$

$$+ 2C_1 \int_{-b_w}^{+b_w} \delta_2(y_d) \int_{-b_w}^{+b_w} m_{1\,\text{opt}}(y)^R \bar{Y} \, dy \, dy_d$$

$$- \int_{-b_w}^{+b_w} \lambda'(y_d) \delta_3(y_d) \, dy_d - C_2 \int_{-b_w}^{+b_w} \delta_1(y_d) \lambda(y_d) g(y_d) \, dy_d$$

$$- C_2 \int_{-b_w}^{+b_w} \delta_2(y_d) \lambda(y_d) g(y_d) \, dy_d = 0 \qquad \text{(A6)}$$

It can be observed that the functions $\delta_1(y_d)$, $\delta_2(y_d)$, and $\delta_3(y_d)$ are arbitrary functions. Thus, it can be written that

$$\delta_2(y_d) = \delta_1(y_d) \equiv 0$$

$$\Rightarrow \int_{-b_w}^{+b_w} \lambda'(y_d) \delta_3(y_d) \, dy_d = 0$$

$$\Rightarrow \lambda'(y_d) = 0 \Rightarrow \lambda(y_d) = \text{cost} \qquad \text{(A7)}$$

Using this result and imposing $\delta_2 \equiv 0$,

$$2C_1 \int_{-b_w}^{+b_w} \delta_1(y_d) \!\!\!\!\not\!\!\!\!\int_{-b_w}^{+b_w} m_{1\,\text{opt}}(y)^S \bar{Y} \, dy \, dy_d$$

$$+ 2C_1 \int_{-b_w}^{+b_w} \delta_1(y_d) \int_{-b_w}^{+b_w} m_{2\,\text{opt}}(y)^R \bar{Y} \, dy \, dy_d$$

$$- C_2 \lambda \int_{-b_w}^{+b_w} \delta_1(y_d) g(y_d) \, dy_d = 0 \tag{A8}$$

The preceding equation can be rewritten as

$$\int_{-b_w}^{+b_w} \delta_1(y_d) 2C_1 \!\!\!\!\not\!\!\!\!\int_{-b_w}^{+b_w} m_{1\,\text{opt}}(y)^S \bar{Y}(y_d, y) \, dy \, dy_d$$

$$+ \int_{-b_w}^{+b_w} \delta_1(y_d) \left[2C_1 \int_{-b_w}^{+b_w} m_{2\,\text{opt}}(y)^R \bar{Y}(y_d, y) \, dy \right.$$

$$\left. - C_2 \lambda g(y_d) \right] dy_d = 0 \tag{A9}$$

Again, the function $\delta_1(y_d)$ is arbitrary. Therefore, in order to solve Eq. (A9), the first Euler–Lagrange equation [relation (9)] has to be satisfied. Operating similarly, imposing $\delta_1 \equiv 0$ and observing that δ_2 is an arbitrary function, the second Euler–Lagrange equation [relation (10)] can be obtained.

Appendix B: Numerical Solution of the Euler–Lagrange Integral Equation

The solution of the system (44) is straightforward.

1) Step 1: The variables are changed in order to have all integrals with endpoints -1 and $+1$. Notice that the singularity in the Hadamard integrals is internal and of order 2. Therefore, the changing of the variables is allowed.[34] Using the transformation,

$$y_d = t b_w, \qquad y = s b_w, \qquad H = h b_w \tag{B1}$$

The system represented by the Euler–Lagrange integral equation and the constraint becomes [see Eq. (44)]

$$\begin{cases} \not\!\!\!\int_{-1}^{+1} \dfrac{m_{\text{opt}}(s)}{(s-t)^2} \, ds + \int_{-1}^{+1} m_{\text{opt}}(s) \dfrac{(s-t)^2 - h^2}{[(s-t)^2 + h^2]^2} \, ds \\ \qquad\qquad - \lambda \cdot 2\pi b_w V_\infty^2 = 0 \\ \bar{L} = -2\rho_\infty b_w \displaystyle\int_{-1}^{+1} m_{\text{opt}}(s) \, ds \end{cases} \tag{B2}$$

2) Step 2: The value of λ is arbitrarily chosen: $\lambda = \lambda_{\text{guess}} \neq 0$. The guessed Lagrange multiplier is not coincident with the real Lagrange multiplyer. Therefore, the solution of the first equation in the system (B2) is not $m_{\text{opt}}(s)$. Let $m_{\text{guess}}(s)$ be called the solution (for now unknown) of the Euler–Lagrange equation [first relation in the system (B2)] corresponding to $\lambda = \lambda_{\text{guess}}$.

3) Step 3: The unknown function $m_{\text{guess}}(s)$ is expanded using a series of known functions. (The unknowns will be the coefficients of such functions.) Suppose the use of the Legendre polynomials. (In this paper this approach is adopted.) Thus, the function $m_{\text{guess}}(s)$ is written as

$$m_{\text{guess}}(s) = \sum_{k=0}^{N-1} c_k P_k(s) \tag{B3}$$

where c_k are the unknown coefficients and $P_k(s)$ are the Legendre polynomials of order k. Substituting this expression into the Euler–Lagrange equation:

$$\sum_{k=0}^{N-1} c_k \!\!\!\!\not\!\!\!\!\int_{-1}^{+1} \dfrac{P_k(s)}{(s-t)^2} \, ds + \sum_{k=0}^{N-1} c_k \int_{-1}^{+1} P_k(s) \dfrac{(s-t)^2 - h^2}{[(s-t)^2 + h^2]^2} \, ds$$

$$- \lambda_{\text{guess}} \cdot 2\pi b_w V_\infty^2 = 0 \tag{B4}$$

4) Step 4: The Euler–Lagrange equation (B4) is solved for a limited number of points (collocation points), which are chosen to be the zeros of the Legendre polynomial $P_N(t)$. Thus, a linear system in the unknown coefficients c_k has to be solved. Considering the lth collocation point t_l [the lth zero of $P_N(t)$], the lth equation of that system is

$$\sum_{k=0}^{N-1} c_k \!\!\!\!\not\!\!\!\!\int_{-1}^{+1} \dfrac{P_k(s)}{(s-t_l)^2} \, ds + \sum_{k=0}^{N-1} c_k \int_{-1}^{+1} P_k(s) \dfrac{(s-t_l)^2 - h^2}{[(s-t_l)^2 + h^2]^2} \, ds$$

$$- \lambda_{\text{guess}} \cdot 2\pi b_w V_\infty^2 = 0 \tag{B5}$$

It is clear that the problem is the numerical evaluation of the integrals. The regular integral does not represent a problem, and it can be calculated using a Gaussian quadrature or an accurate adaptive quadrature formula. The Hadamard integral requires special attention (see Appendix C).

5) Step 5: Once the linear system is solved, the coefficients c_k are found, and the function $m_{\text{guess}}(s)$ is then calculated using Eq. (B3). The function $m_{\text{guess}}(s)$ is substituted into the constraint equation [second relation in Eq. (B2)]. The integral is a standard integral and can be calculated using a Gaussian quadrature formula. The constraint is, in general, not satisfied and, therefore, instead of $\bar{L}$, $\bar{L}_{\text{guess}}$ is found:

$$\bar{L}_{\text{guess}} = -2\rho_\infty b_w \int_{-1}^{+1} m_{\text{guess}}(s) \, ds \tag{B6}$$

6) Step 6: Because of the linearity of the Euler–Lagrange equation, it can be concluded that

$$m_{\text{opt}}(s) = (\bar{L}/\bar{L}_{\text{guess}}) m_{\text{guess}}(s) \tag{B7}$$

General Case with More Unknowns and Multiple Constraints

The biplane with the constraint of fixed lift is only a particular case. In the general case, the lifting line is described with more than one equation. For example, consider a box wing obtained by joining the upper and lower wing of a biplane: the lifting line is divided into four different parts, and the distribution on each part is an unknown. Also, the constraints can be more than just the total lifting force. For example, the root moment or the weight can be considered as additional constraints. How this problem is handled is explained next.

Consider again the system (B2), valid for a biplane with a single constraint (the total lift). Suppose that the unknown optimal distribution m_{opt} is written as a combination of Legendre's polynomials [similar to Eq. (B3)]. Applying the collocation method, the system represented by the Euler–Lagrange equation (this equation is satisfied in the collocation points; therefore, N equations are written) and the constraint can be written in the following compact form:

$$\begin{cases} a_{kl} c_k - \lambda \cdot 2\pi b_w V_\infty^2 \delta_l = 0_l \\ \qquad\qquad k = 0, N-1; \, l = 1, N; \, \delta_l = 1; \, 0_l = 0 \\ c_k b_k = \bar{L} \end{cases} \tag{B8}$$

Notice that the quantities b_k and a_{kl} are the integrals of the Legendre polynomials multiplied by some functions (regular or singular, and in the last case the integrals are Hadamard finite-part integrals). In a matrix form, the preceding equation is written as

$$\begin{cases} \boldsymbol{A} \cdot \boldsymbol{c} - \lambda \cdot 2\pi b_w V_\infty^2 \boldsymbol{\delta} = \boldsymbol{0} \\ \boldsymbol{b}^T \cdot \boldsymbol{c} = \bar{L} \end{cases} \tag{B9}$$

The matrix $\boldsymbol{A}$ and the vectors $\boldsymbol{\delta}$ and $\boldsymbol{b}$ are known, and their definition is obvious from Eq. (B8). The unknowns are the vector $\boldsymbol{c}$ of the coefficients of the Legendre polynomials and the Lagrange multiplier λ.

The system (B9) can be written in a more concise form if the Lagrange multiplier λ is included in the vector of unknowns. Defining $\mathcal{X}$ as the vector of the new unknowns (vector $\mathbf{c}$ and Lagrange multiplier), Eq. (B9) can be rewritten as

$$\mathcal{A} \cdot \mathcal{X} = \mathcal{L} \tag{B10}$$

Notice that $\mathcal{A}$ is a $(N+1) \times (N+1)$ matrix and $\mathcal{L}$ is a known vector. By solving the preceding system, the coefficients of the unknown optimal distribution and the Lagrange multiplier can be found. It has to be clear that this method is equivalent to the method explained in steps 1 through 6. However, this is more general and can be used in the case with more than one unknown distribution and multiple constraints.

The general case is more complex because the unknown distribution can be split into several parts and more constraints (here, only linear constraints in the doublet distributions are considered) can be applied. However, the Euler–Lagrange equations can be obtained by using the procedure already explained. The fact that more constraints are applied implies that more Lagrange multipliers have to be considered. But using the method that allowed the writing of Eq. (B10), it is possible to solve a linear system and calculate the coefficients of the Legendre polynomials and the Lagrange multipliers.

Appendix C: Hadamard Finite-Part Integrals—Quadrature Formula

In this section, a particular quadrature formula for the Hadamard finite-part integrals[33−35] is described. Consider the following hypersingular integral:

$$I_{lk}^{Had} = \fint_{-1}^{+1} \frac{P_k(s) g_1(t_l, s)}{(s - t_l)^2} \, ds \tag{C1}$$

Notice that in Eq. (B5) the function $g_1(t_l, s)$ is 1. The integral I_{lk}^{Had} can be calculated using a particular quadrature formula[34]:

$$I_{lk}^{Had} = \fint_{-1}^{+1} \frac{P_k(s) g_1(t_l, s)}{(s - t_l)^2} \, ds = \sum_{i=1}^{M} w_i^I(t_l) \frac{P_k(s_i) g_1(t_l, s_i)}{(s_i - t_l)^2} \tag{C2}$$

The last relation contains the following quantities:

1) The nodes s_i coincide with the zeros of the Legendre polynomial $P_M(s)$. Notice that in general $M \neq N$. Several numerical tests[32] have been performed, and a good choice for the problems analyzed in this paper is represented by $N = 20$ and $M = 200$.

2) The weights are

$$w_i^I(t_l) = h_i \sum_{j=0}^{M-1} d_j^{-1} P_j(s_i) [Q_j'(t_l)]$$

3) The Gauss weights h_i are also included.
4) The integrals of the square of the Legendre polynomials are

$$d_j = \int_{-1}^{+1} P_j^2(s) \, ds = \frac{2}{2j+1}$$

5) The derivative of the integrals interpreted in the Cauchy sense is

$$Q_j'(t_l) = \frac{d}{dt_l} Q_j(t_l) = \frac{d}{dt_l} \fint_{-1}^{+1} \frac{P_j(s)}{s - t_l} \, ds$$

The Hadamard finite-part integrals can be seen as derivative of the Cauchy integrals. Thus, it is obvious that in the quadrature formula Cauchy integrals appear as well.
Expressing Q_j and their derivatives:

$$Q_0(t_l) = \fint_{-1}^{+1} \frac{1}{s - t_l} \, ds = -\ln(1 + t_l) + \ln(1 - t_l)$$

Operating in a similar way,

$$Q_1(t_l) = \lim_{\varepsilon \to 0} \left(\int_{-1}^{t_l - \varepsilon} \frac{s}{s - t_l} \, ds + \int_{t_l + \varepsilon}^{+1} \frac{s}{s - t_l} \, ds \right)$$

$$\Rightarrow Q_1(t_l) = [1 + t_l \ln(1 - t_l)] - [-1 + t_l \ln(1 + t_l)]$$

A recursive formula is possible to use to determine the quantities $Q_j(t_l)$ and $Q_j'(t_l)$ as follows:

$$Q_j(t_l) = (a_j t_l + b_j) Q_{j-1}(t_l) - c_j Q_{j-2}(t_l) \tag{C3}$$

where $a_j = (2j-1)/j$, $b_j = 0$, $c_j = (j-1)/j$. The final expressions for the integrals interpreted in the Cauchy principal value sense can be written as

$$Q_j(t_l) = t_l[(2j-1)/j] Q_{j-1}(t_l) - [(j-1)/j] Q_{j-2}(t_l)$$

$$Q_j'(t_l) = t_l[(2j-1)/j] Q_{j-1}'(t_l) - [(j-1)/j] Q_{j-2}'(t_l)$$

$$+ [(2j-1)/j] Q_{j-1}(t_l) \tag{C4}$$

This equation leads to calculating the weights $w_i^I(t_l)$ and, as a result, the integral I_{lk}^{Had}. All of these derivations are valid because the singularity is contained in the integration domain. If this is not true, different formulas have to be considered, and the changing of variables has to be done carefully.[34]

Appendix D: Optimal Doublet Distribution in a Classical Cantilevered Wing

In a cantilevered wing, it is well known that the optimal circulation distribution is elliptical. Here the optimal distribution can be found using the tools illustrated in the paper. Suppose that the doublets axes are directed along $-z$. Applying the described procedure (the coefficients of lift and induced drag are obtained by dividing the lift and induced drag by $\frac{1}{2} \rho_\infty V_\infty^2 2 b_w l$), the coefficients of lift and induced drag are written in terms of the doublet distribution as

$$C_{D_i} = -\frac{1}{4\pi V_\infty^4 b_w l} \int_{-b_w}^{+b_w} m(y) \fint_{-b_w}^{+b_w} \frac{m(y_d)}{(y - y_d)^2} \, dy_d \, dy$$

$$C_L = \frac{1}{V_\infty^2 b_w l} \int_{-b_w}^{+b_w} m(y) \, dy \tag{D1}$$

Using the methods applied in the biplane, the Euler–Lagrange equation becomes

$$\frac{1}{2\pi V_\infty^2} \fint_{-b_w}^{+b_w} \frac{m_{opt}(y)}{(y - y_d)^2} \, dy + \lambda = 0 \tag{D2}$$

With the constraint represented by the coefficient of lift,

$$\bar{C}_L = \frac{1}{V_\infty^2 b_w l} \int_{-b_w}^{+b_w} m_{opt}(y) \, dy \tag{D3}$$

The fact that the optimal distribution is elliptical can be verified by using an elliptical distribution written in the form

$$m_{opt}(y) = \bar{m} \sqrt{1 - y^2 / b_w^2} \tag{D4}$$

Notice that the chosen distribution is exactly zero at both tips of the wing (the endpoints of the Hadamard integral). This is because the circulation {which is related to the doublet distribution by a constant factor [see Eq. (33) obtained for the doublets with axes in the $+z$ direction]} has to be zero at such points. Moreover, because the doublet distribution has the property just mentioned, the Hadamard integral has the singularity point always included in the interval of integration, and this simplifies the mathematical calculation of

it.[34] Substituting Eq. (D4) into Eqs. (D2) and (D3) and using the substitutions $y = b_w s$ and $y_d = b_w t$, the system becomes

$$\begin{cases} \dfrac{\bar{m}}{2\pi b_w V_\infty^2} \fint_{-1}^{+1} \dfrac{\sqrt{1-s^2}}{(s-t)^2}\, \mathrm{d}s + \lambda = 0 \\[2mm] \bar{C}_L = \dfrac{\bar{m}\pi}{2V_\infty^2 l} \end{cases} \tag{D5}$$

The Hadamard integral is known[35]:

$$\fint_{-1}^{+1} \frac{\sqrt{1-s^2}}{(s-t)^2}\, \mathrm{d}s = -\pi \tag{D6}$$

Thus, the system represented by the Euler–Lagrange equation and the constraint becomes

$$\begin{cases} -\dfrac{\bar{m}}{2\pi V_\infty^2 b_w}\pi + \lambda = 0 \Rightarrow \lambda = \dfrac{\bar{C}_L l}{\pi b_w} \\[2mm] \bar{m} = \dfrac{2V_\infty^2 l}{\pi}\bar{C}_L \end{cases} \tag{D7}$$

The system is satisfied, and, thus, the distribution $m_{\mathrm{opt}}(y) = \bar{m}\sqrt{(1 - y^2/b_w^2)} = (2V_\infty^2 l/\pi)\bar{C}_L\sqrt{(1 - y^2/b_w^2)}$ is the optimal distribution.

It has been proved that if the distribution is elliptical [see Eq. (D4)], the following relations are valid:

$$\fint_{-b_w}^{+b_w} \frac{m_{\mathrm{opt}}(y)}{(y - y_d)^2}\, \mathrm{d}y = -\bar{m}\frac{\pi}{b_w}, \qquad \int_{-b_w}^{+b_w} m_{\mathrm{opt}}(y)\, \mathrm{d}y = \bar{m}\frac{b_w \pi}{2} \tag{D8}$$

Substituting Eq. (D8) into Eq. (D1), the coefficient of the minimum induced drag can be found:

$$\left(C_{D_i}\right)_{\mathrm{opt}} = -\frac{1}{4\pi V_\infty^4 b_w l}\int_{-b_w}^{+b_w}\left[m_{\mathrm{opt}}(y)\left(-\bar{m}\frac{\pi}{b_w}\right)\right]\mathrm{d}y$$

$$= \frac{\pi}{8 b_w V_\infty^4 l}\bar{m}^2 = \frac{\pi}{8 b_w V_\infty^4 l}\left(\frac{2V_\infty^2 l}{\pi}\bar{C}_L\right)^2 = \frac{l\bar{C}_L^2}{2 b_w \pi} \tag{D9}$$

Instead of working with the coefficients of lift and induced drag, it is possible to work with the lift and induced drag. This is useful for the comparison with the biplane (because such comparison is done using the same lift force). Remembering the relations

$$(D_i)_{\mathrm{opt}} = \tfrac{1}{2}\rho_\infty V_\infty^2 2 b_w l\left(C_{D_i}\right)_{\mathrm{opt}}, \qquad \bar{L} = \tfrac{1}{2}\rho_\infty V_\infty^2 2 b_w l\bar{C}_L \tag{D10}$$

it is possible to write

$$\bar{m} = 2\bar{L}/(\rho_\infty \pi b_w) \qquad (D_i)_{\mathrm{opt}} = \bar{L}^2 / \left(2\pi\rho_\infty b_w^2 V_\infty^2\right) \tag{D11}$$

Acknowledgments

References

[1]Prandtl, L., and, Tietjens, O. G., *Applied Hydro and Aeromechanics*, Dover, New York, pp. 203–222.

[2]Munk, M., "Isoperimetric Problems from the Theory of Flight," Inaugural Dissertation, Gottingen, Germany, 1919 (in German).

[3]Kroo, I., "Drag due to Lift: Concepts for Prediction and Reduction," *Annual Reviews Fluid Mechanics*, Vol. 33, 2001, pp. 587–617.

[4]Mortara, K., Straussfogel, D. M., and Maughmer, M. D., "Analysis and Design of Planar and Non-Planar Wings for Induced Drag Minimization," NASA-CR-189509, Annual Progress Report, 1991.

[5]Smith, S. C., "A Computational and Experimental Study of Nonlinear Aspects of Induced Drag," NASA Technical Paper 3598, Feb. 1996.

[6]Anderson, J., *Fundamentals of Aerodynamics*, McGraw–Hill, New York, 1991.

[7]Pistolesi, E., "Betrachtungen über die Gegenseitige Beeinflussung von Tragflügelsystemen," Gesammelte Vorträge der Hauptversammlung, Lilienthal-Gesellschaft, Berlin, 1937.

[8]Weissinger, J., "Über die Auftriebverteilung von Pfeilflügeln," Forschungsbericht der Berliner Zentrale fur wissenschaftliches Berichtswesen, 1553, Berlin-Adlershof, 1942.

[9]Weissinger, J., "The Lift Distribution of Swept-Back Wings," NACA TM 1120, March 1947.

[10]Eppler, E., "Die Entwicklung der Tragflügeltheorie," *Zeitschrift für Flugwiss*, Nov. 1987, pp. 133–144.

[11]Prandtl, L., "Applications of Modern Hydrodynamics to Aeronautics," NACA Report 116, June 1921.

[12]Falkner, V. M., "The Calculation of Aerodynamic Loading on Surfaces of Any Shape," Aeronautical Research Council, R&M, London, 1910, 1943.

[13]Schlichting, H., and Thomas, H. H. B. M., "Note on the Calculation of the Lift Distribution of Swept Wings," R.A.E., Report AERO 2236, 1947.

[14]Robinson, A., and Laurmann, M. A., *Wing Theory*, Cambridge Univ. Press, Cambridge, England, UK, 1956.

[15]Schlichting, H., and Truckenbrodt, E., *Aerodynamics of the Airplane*, McGraw–Hill, New York, 1979.

[16]Jones, R. T., and Cohen, D., *High-Speed Wing Theory*, Princeton Univ. Press, Princeton, NJ, 1960.

[17]Mittelman, Z., "Prediction of Unsteady Aerodynamics and Control of Delta Wings with Tangential Leading Edge Blowing," Ph.D. Dissertation, SUDDAR 580, Dept. of Aeronautics and Astronautics, Stanford Univ., CA, June 1989.

[18]Quackenbush, T. R., Bliss, D. B., Wachspress, D. A., and Ong, C. C., "Free Wake Analysis of Hover Performance Using a New Influence Coefficient Method," NASA CR-4150, July 1988.

[19]Lamb, H., *Hydrodynamics*, 6th ed., Dover, New York, 1945.

[20]Ramachandran, K., Tung, C., and Caradonna, F. X., "The Free-Wake Prediction of Rotor Hover Performance Using a Vortex-Embedding Method," AIAA Paper 89-0638, Jan. 1989.

[21]Nagati, M. G., Iverson, J. D., and Vogel, J. M., "Vortex Sheet Modeling with Curved Higher-Order Panels," *Journal of Aircraft*, Vol. 24, No. 11, 1987, pp. 776–782.

[22]Ribeiro, R. S., "Analysis of Wing Wake Roll-up Using a Vortex-in-Cell Method," Ph.D. Dissertation, Dept. of Aeronautics and Astronautics, Stanford Univ., CA, May 1992.

[23]Albano, E., and Rodden, W., "A Doublet Lattice Method for Calculating Lifting Distributions on Oscillating Surfaces in Subsonic Flows," *AIAA Journal*, Vol. 7, No. 2, 1969, pp. 279–285.

[24]Katz, J., and Plotkin, A., *Low-Speed Wing Aerodynamics*, McGraw–Hill, New York, 1991.

[25]Maskew, B., "Prediction of Subsonic Aerodynamic Characteristics: A Case for Low-Order Panel Methods," *Journal of Aircraft*, Vol. 19, No. 2, 1982, pp. 157–163.

[26]Ashenberg, J., and Weihs, D., "Minimum Induced Drag of Wings with Curved Planform," *Journal of Aircraft* , Vol. 21, No. 1, 1984, pp. 89–91.

[27]Butter, D. J., and Hancock, G. J., "A Numerical Method for Calculating the Trailing Vortex System Behind a Swept Wing at Low Speed," *The Aeronautical Journal of the Royal Aeronautical Society*, Vol. 75, Aug. 1971, pp. 564–568.

[28]Smith, S. C., "A Computational and Experimental Study of Nonlinear Aspects of Induced Drag," Ph.D. Dissertation, Dept. of Aeronautics and Astronautics, Stanford Univ., CA, June 1995.

[29]Kroo, I., and Smith, S. C., "Computation of Induced Drag with Nonplanar and Deformed Wakes," Society of Automotive Engineering, 901933, Warrendale, PA, Sept. 1990.

[30]Bacciotti, A., "Teoria Matematica dei Controlli," CELID Turin, Italy, 1998, Chaps. 9–12.

[31]Reddy, J. N., *Energy and Variational Methods in Applied Mechanics*, Wiley, New York, 1984.

[32]Demasi, L., "Aerodynamic Analysis of Non-Conventional Wing Configurations for Aeroelastic Applications," Ph.D. Dissertation, Dipartimento di Ingegneria Aeronautica e Spaziale, Torino, Italy, March 2004.

[33]Hadamard, J., *Lectures on Cauchy's Problem in Linear Partial Differential Equations*, Yale Univ. Press, New Haven, CT, 1952.

[34]Monegato, G., "Numerical Evaluation of Hypersingular Integrals," *Journal of Computational and Applied Mathematics*, Vol. 50, Nos. 1-3, 1994, pp. 9–31.

[35]Kaya, A. C., and Erdogan, F., "On the Solution of Integral Equations with Strongly Singular Kernels," NASA-CR-178138, June 1986.

[36]Demasi, L., "Ala Anulare Ellittica: Distribuzione di Circolazione di Minima Resistenza Indotta," *Proceedings of the Italian Conference AIDAA*, Sept. 2003.

[37]Frediani, A., Montanari, G., and Pappalardo, M., "Sul Problema di Prandtl della Minima Resistenza Indotta di un Sistema Portante," *Proceedings of the 15th National Italian Conference AIDAA*, Nov. 1999.

[38]Prandtl, L., "Induced Drag of Multiplanes," NACA TN 182, Feb. 1924.

[39]Munk, M., "The Minimum Induced Drag in Airfoils," NACA, Report 121, 1921.

[40]Prandtl, L., "Beitrag zur Theorie der Tragenden Fläche," *ZAMM*, Vol. 16, No. 6, 1936, pp. 360, 361.

[41]Demasi, L., Chiocchia, G., and Carrera, E., "Aerodinamica dei Sistemi Portanti Chiusi: ala Anulare Ellittica," *Proceedings of the 17th National Italian Conference AIDAA*, Sept. 2003.

[42]Jones, R. T., "The Spanwise Distribution of Lift for Minimum Induced Drag of Wings Having a Given Lift and a Given Bending Moment," NACA TN 2249, Dec. 1950.

[43]Kroo, I., "A General Approach to Multiple Lifting Surface Analysis and Design," AIAA Paper 84-2507, Oct. 1984.

[44]Cone, C., "Theory of Induced Lift and Minimum Induced Drag of Nonplanar Lifting Systems," NASA TR R-139, Jan. 1962.